Int. J. Heat Mass Transfer. Vol. 13, pp. 789–807. Pergamon Press 1970. Printed in Great Britain

THERMAL CONTACT RESISTANCE: THE DIRECTIONAL EFFECT AND OTHER PROBLEMS

T. R. THOMAS* and S. D. PROBERT

School of Engineering, University College, Swansea, U.K.

(*Received* 29 *July* 1969 *and in revised form* 4 *November* 1969)

Abstract—Areas of uncertain knowledge in the field of thermal contact resistance are described. A theory for the variation of contact resistance with load based on recent advances in surface topography analysis is outlined, and existing theories for the so-called directional effect are critically discussed. The construction and use of an apparatus to measure the variation of thermal conductance with various parameters at temperatures from 300°K downwards is described, and results for contact combinations of stainless steel and aluminium specimens presented. Agreement between theoretical prediction and experimental observation is fair for random surfaces but breaks down for surfaces with lay. Directional effects have been found for a contact between similar materials; an attempt is made to account for this on the basis of a previous electronic theory for the effect.

NOMENCLATURE

- A, nominal contact area [cm^2];
- a, radius of microscopic contact spot [cm];
- b, radius of cylindrical specimen [cm];
- C, thermal conductance/unit area [W/cm^2 °K];
- E, elastic modulus [kg/cm^2];
- k, thermal conductivity [W/cm °K];
- ℓ, Boltzmann's constant [J/°K];
- l, land length [cm];
- M, projected surface hardness [kg/mm^2];
- n, number of contacts;
- P, applied pressure [kg/cm^2];
- p, period [h];
- $\dot{Q}$, rate of heat transfer [W];
- R, thermal resistance/unit area [cm^2 °K/W];
- T, temperature [°K];
- t, u/σ;
- u, separation of mean planes [μ];
- v, radius of macroscopic contact spot [cm];
- α, $\tan^{-1}\gamma$;
- β, angle between profile and surface lay [rad];
- γ, ratio of length-to-breadth of contact spot;
- δ, linear expansion coefficient [°K^{-1}];
- ε, work function [eV];
- θ, base angle of surface cones [rad];
- λ, plasticity index;
- ν, Poisson's ratio;
- ρ, radius of curvature [μ];
- σ, standard deviation of surface height: RMS roughness [μ];
- τ, transmissivity;
- Ψ, $|\bar{\psi}|/\sigma$ [cm^{-1}];
- ψ, surface slope [rad];
- ω, constant relating hardness and time.

Subscripts

- A, per unit area;
- AL, aluminium;
- D, in downward direction;
- EM, steel;
- $i(=1, 2)$, for metal i;

* Present address: Burndy Corporation, Norwalk, Connecticut, U.S.A.

L, per unit length;
o, for the oxide film;
p_i, after period p_i ($i = 1, 2$);
s, of the solid;
U, in upward direction;
β, at angle β to lay of surface.

Prefix
Δ, small change of.

INTRODUCTION

In recent years considerable attention has been given to the subject of thermal contact resistance. However a notable feature of the published work has been the very wide discrepancies between experimental results of different investigators using nominally similar materials. Also each of the theories that has been advanced generally can be applied only to the experimental results of the investigator proposing that particular theory.

The present work was an attempt to obtain accurate experimental measurements under strictly controlled conditions which would allow a fairly rigorous application of theory. In addition experimental information was sought on two problems of technological interest: the behaviour of thermal contact resistance at cryogenic temperatures, and the so-called directional or thermal-rectifying effect.

THEORY

The thermal contact conductance C per unit area of an interface of nominal area A, across which a temperature drop ΔT exists is defined by

$$C = \dot{Q}/A\Delta T \qquad (1)$$

where $\dot{Q}$ is the total rate of heat flow. The thermal resistance equals the reciprocal of C. This resistance arises from the fact that under moderate loads the surfaces are in intimate contact only at a number of small discrete spots, and the amount of heat passing through these is reduced still further by the constriction of the lines of flow. The usual approach to the problem is to consider a model interface of small circular constrictions far apart, each fed by a circular channel independently of the others. If heat transfer through the interstitial medium is neglected (corresponding to the practical case of a vacuum environment of better than 5×10^{-6} torr with boundaries at less than 40°K) the problem is analogous to that for electrical contact solved by Holm [1] and the solution is

$$C = 2an_A k_s \qquad (2)$$

where a is the contact spot radius, n_A the number of contacts per unit area and k_s the harmonic mean thermal conductivity of the contact members.

The above model is a reasonable approximation to the contact between two "flat" surfaces one or both of which are randomly rough. The mechanical behaviour of such a contact under load has been discussed by Tsukizoe and Hisakado [2, 3]. They considered a surface consisting of randomly intersecting cones of base angle θ with a normal distribution of surface heights, and assumed that asperity deformation is entirely plastic. Making the additional assumption that θ is small, their expressions reduce to

$$\bar{n}_A = \pi\Psi^2 t\phi(t)/8 \qquad (3)$$

$$\bar{a} = 2/\pi\Psi t \qquad (4)$$

and

$$\bar{n}_L = \Psi\phi(t)/2 \qquad (5)$$

where
$\Psi = |\bar{\psi}|/\sigma$, the ratio of the mean absolute profile slope (see Fig. 1) to the R.M.S. roughness and the bars denote average values. Also

$$\phi(t) = \frac{1}{\sqrt{2\pi}} \exp\left(-\frac{t^2}{2}\right).$$

The relation to the dimensionless load is given by

$$\frac{P}{M} = \frac{1}{2} - \int_0^t \phi(t)\,dt \qquad (6)$$

where P = apparent pressure
and M = hardness of the softer surface.
Substituting (3) and (4) in (2) gives

$$C = \Psi\phi(t)\,k_s/2. \tag{7}$$

Greenwood [4] developed a simple test for the deformation mechanism: a plasticity index $\lambda = (E^*/M)\sqrt{(\sigma/\bar{\rho})}$ was defined, where

$$1/E^* = (1 - \nu_1^2)/E_1 + (1 - \nu_2^2)/E_2 \tag{8}$$

E_i and ν_i are the elastic modulus and Poisson's ratio respectively for metal i, and $\bar{\rho}$ is the mean peak radius of curvature (see Fig. 1). For $\lambda > 1$ the surfaces will deform plastically, while for $\lambda < 0{\cdot}7$ the deformation will be elastic.

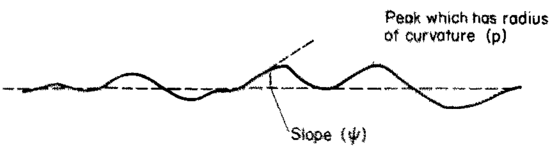

FIG. 1. Terminology for a surface profile.

DIRECTIONAL EFFECT

The so-called directional effect refers to a curious property of certain contacts by which they have a greater thermal resistance in one direction across the contact than in the reverse direction. The effect was first noted by Starr [5] and has subsequently been reported by several others [6–12]. Some of the hypotheses advanced to explain the phenomenon have relied upon a change in contact geometry caused by differential thermal expansion. In the majority of reported incidences the contacts have been between dissimilar materials, usually steel and aluminium, and Clausing [10] and Barber [13] have argued that no directional effect can occur between specimens of the same material. In Appendix 1 their arguments are shown to be incomplete: a directional effect between specimens of the same material was in fact observed by Williams [9].

Another explanation was proposed by Moon and Keeler [14], who suggested that the directional effect is due to the potential barrier produced by the interfacial oxide layers, which inhibit the electronic heat flow. If ε_1 and ε_2 are the work functions of the metal surfaces and $\varepsilon_1 > \varepsilon_2$, electrons will flow from metal 2 to metal 1 since the electrons in the conduction band of metal 2 are nearer the top of the potential barrier.

The ratio of the conductances in the direct and reversed directions can be expressed as

$$\frac{C_{12}}{C_{21}} = \frac{\tau_{12}}{\tau_{21}}\frac{T_1^2}{T_2^2}\exp\left\{\left(\frac{\varepsilon_1 - \varepsilon_0}{k}\right)\left(\frac{1}{T_2} - \frac{1}{T_1}\right)\right\} \tag{9}$$

where τ = transmissivity, ε_0 = work function of oxide film and k = Boltzmann's constant. It is stated that $\tau_{12} \simeq \tau_{21}$ and $\varepsilon_1 > \varepsilon_0$: if $T_1 > T_2$, then $C_{12} > C_{21}$. Work functions are sensitive to the state and preparation of the surfaces, hence there is no reason why a directional effect should not occur between similar materials if the surface histories are different.

Powell *et al.* [15] failed to find a directional effect with their thermal comparator. With this device the rate of change of temperature of a small metal sphere placed in contact with the test surface was observed. They concluded that the directional effect is due to specimen geometry rather than to a potential barrier and that their failure to observe it was because of the small contact area used. A possible alternative explanation is that the oxide film was usually broken and metal-to-metal contact achieved over this very small contact region ($\sim 5{\cdot}5 \times 10^{-5}$ cm^2 at the highest load).

EXPERIMENTAL RIG

The thermal conductance apparatus consisted of a cryostat (Fig. 2) designed to operate from room temperature down to 4°K by immersion in liquid refrigerants, together with associated vacuum systems and instrumentation. Cryostats for the measurement of thermal properties under load have been discussed previously [16, 17], the present design being a development

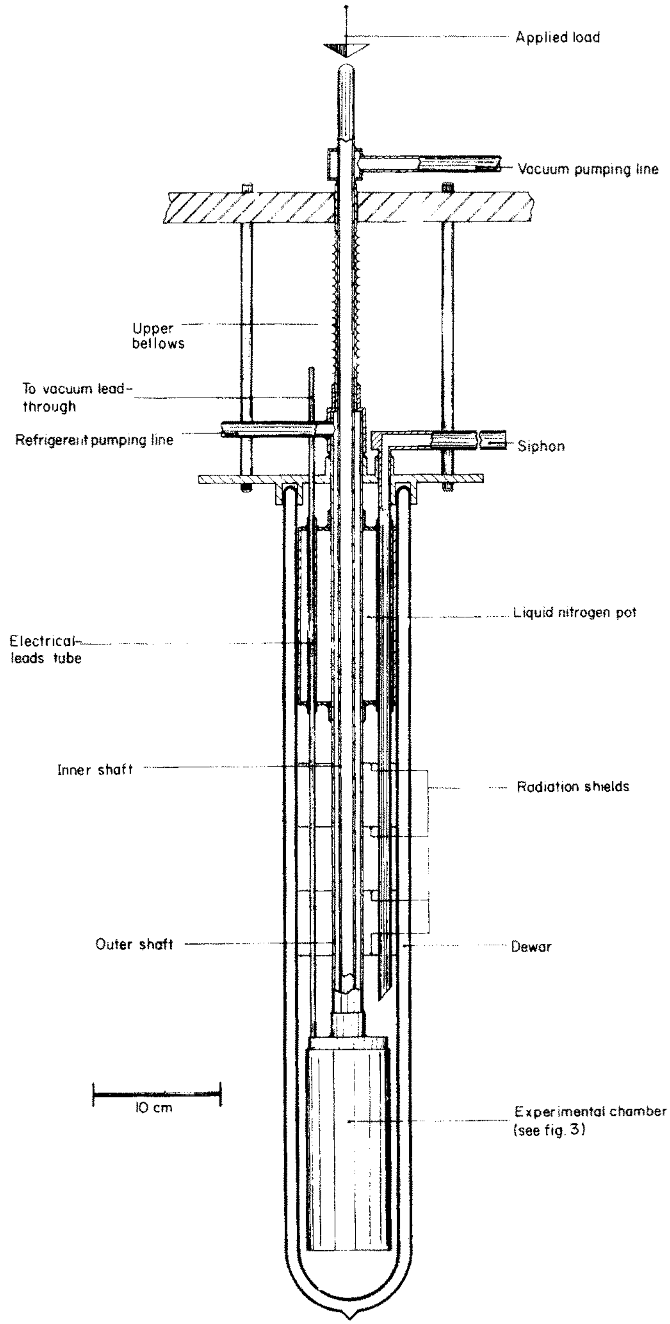

FIG. 2. Schematic representation of the cryostat.

of that of Zavaritskii [18]. Loads of up to 100 kg could be applied kinematically to the contact interface and heat flows of up to 3 W could be reversed without disturbing the specimens (see Fig. 3). The heaters were energized by stabilized d.c. power supplies. The load was applied by a lever and hanging weight arrangement which was calibrated with a quartz load cell. The experimental chamber could be evacuated to 10^{-6} torr, and a facility existed for bleeding in helium "exchange" gas.

In case the variation of contact resistance was highly temperature dependent, the apparatus was designed to work with very small axial temperature gradients along the specimens. Each copper–constantan thermocouple circuit was independent, being insulated from the others and from the specimens. All the measuring circuits were screened, and e.m.f.'s were determined to 10^{-7} V with a precision potentiometer system. The thermocouples were all made from the same batches of 0·12 mm dia. wire: the largest dimension of the hot junction being two diameters. The thermocouples were calibrated during a separate experiment and cemented into the specimens with an aluminium-filled epoxy resin.

The heat flux was measured by using the specimens as their own heat meters, their thermal conductivities having previously been measured (see Fig. 4).

THE SPECIMENS

Two materials were used; stainless steel as specified by En. 58F (M), which is similar to the AISI 302/304 used by other investigators in this

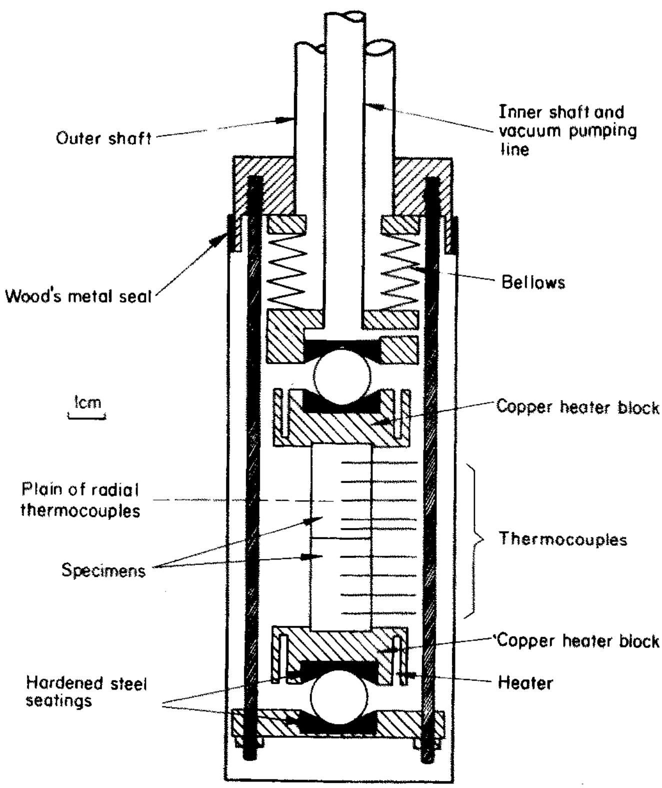

FIG. 3. Schematic section of the experimental chamber.

field, and aluminium as specified by BS He 20. Four specimens were made, three of steel and one of aluminium, and each was turned to a nominal length and diameter of 2·5 and 1·5 cm respectively. Four thermocouple holes of 0·5 mm dia. were drilled radially onto the axis of each specimen at 0·5 cm axial intervals; these holes were offset at 60° angles consecutively in order to minimize the cumulative perturbation to the heat flux. In two of the steel specimens an additional three radial holes were drilled, one onto the axis at 0·25 cm from the interface to monitor constriction perturbations, the others at 1 cm from the interface drilled to depths of two-thirds and one-third of the radius respectively and set at 60° to each other and to the axial thermocouple in order to monitor radial temperature gradients. Specimen dimensions and positions of thermocouple wells were measured to 10^{-4} cm with an optical comparator.

All the specimens were initially lapped optically flat at the interface end. Two of the steel specimens were then shot-blasted with glass beads so that randomly rough surfaces were produced. The remaining steel specimen was used, as lapped, for one series of experiments and subsequently ground to give a surface with directional properties. Vickers microhardness tests were made on the lapped surfaces of each material including a check, with a negative result, for radial gradients in hardness. The dependence of hardness upon temperature as shown in Fig. 5 and used in this work, is based on a compilation of data given by Durham *et al.* [19] for similar materials. Surface profiles of all the rough surfaces were recorded on paper tape using a Talysurf 4 and data logger, and values for the mean absolute slope, RMS roughness and mean peak radius of curvature were obtained by computer analysis. This part of the work is described more fully elsewhere [20].

EXPERIMENTAL PROCEDURE

After assembly of the specimens the vacuum can was soldered in position and the experimental chamber evacuated. An appropriate

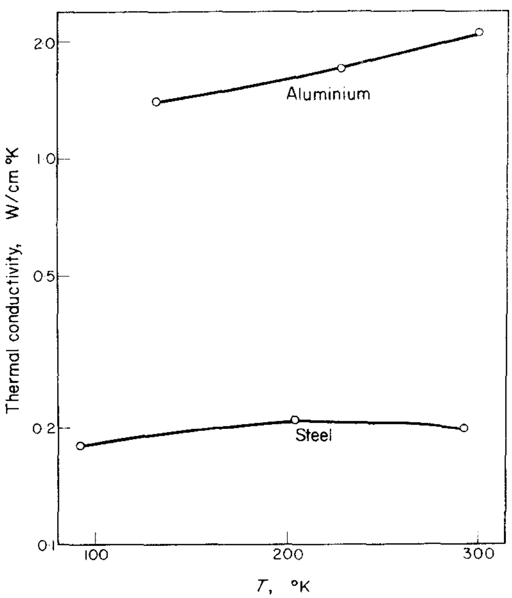

FIG. 4. Thermal conductivity measurements.

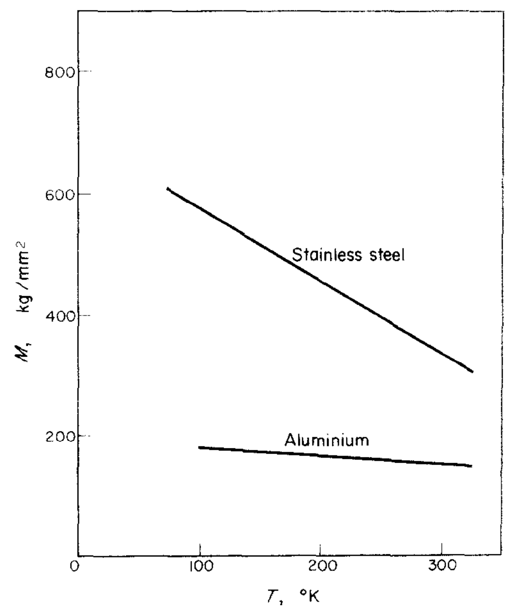

FIG. 5. Hardness of the specimens.

Table 1. Specimen parameters

Specimen	Material	Finish	$\sigma(\mu)$	$\lvert\bar{\psi}\rvert$ (degrees)	$\bar{\rho}(\mu)$
EM1	stainless steel	lapped	—	—	—
EM2	stainless steel	bead-blasted	1·43	6·2	20
EM3	stainless steel	bead-blasted	1·40	6·3	24
EM1′	stainless steel	ground	0·60	3·4*, 4·3†	26*, 19†
AL3	aluminium	lapped	—	9·4	20

* $\beta = \pi/4$.
† $\beta = \pi/2$.

liquid was introduced into the surrounding Dewar flask: for room temperature measurements, this was water, circulated from the mains; for lower temperatures, either a CO_2/acetone mixture maintaining a temperature of 195°K or liquid nitrogen at 77°K was used. A heater was then switched on and the apparatus was left overnight to attain a steady state. For measurements in vacuo, readings were commenced at an indicated pressure of 5×10^{-5} torr or below. At room temperatures, a steady state was regained in 4–5 h after a change of load, and in 10–12 h after a change in heat flow direction: at cryogenic temperatures these times were approximately halved.

A computer program was written in order (i) to fit the best straight lines by a least squares analysis to the temperature gradients in each specimen, (ii) to extend these lines to the interface, taking into account the uncertainty involved in the extrapolation [21] and hence (iii) to calculate the heat fluxes and thermal conductances. Calibration polynomials for the thermocouples and the loading system were also embodied in the program, as were the temperature variations of the thermal conductivities. A detailed error analysis was printed out for each result. In many cases more than one observation was taken under the same experimental conditions; in such cases the observa-

Table 2. The specimen pair combinations tested and the sequence of the experiments

Specimen pair	Upper specimen	Lower specimen	Order of experiments: Parameter varied	Order of experiments: Temperature region (°K)
A	EM1	EM3	time	300
			heat flux	300
			heat flow direction	300
			load	300
			heat flow direction	90*
			temperature	90–300
			load	300
			ambient pressure	300
B	EM3	EM2	load	300
			load	90
			load	130
			load	200
C	EM1′	AL3	load	300
			load	230
			load	150

* Specimens disassembled (i.e. contact broken) after this experiment.

tions have been combined to reduce the error, and the total number of observations is given on the appropriate figure.

Heat fluxes in the axial direction for the two contacting specimens generally agreed to within 10 per cent. Larger discrepancies were sometimes noted, particularly at low temperatures, and were apparently associated with radial temperature gradients in the vicinity of the contact. The instrumentation of the radial thermocouples was not reliable enough, however, to yield quantitative information on this.

RESULTS

Specimen pair A

The first measurements made with specimen pair A were of the variation of room temperature conductance with time, all other parameters being held constant. This was firstly to check the reproducibility of results and secondly to investigate a periodic variation of conductance with time of up to 25 per cent with a period of ~2 h that had been reported by Clausing [22]. No such variation was found (see Fig. 6), but a definite though small increase in conductance with time was noted. Similar increases have been remarked upon by Barzelay *et al.* [6], Boeschoten [23], Forster, as quoted by Skipper and Wootton [24], and Cordier [25]. All the parameters upon which the thermal contact conductance is believed to depend are time-invariant except for the surface hardness. Cetinkale and Fishenden [26] found experimentally that

$$M = M_{p_0}(1 - \omega \log_e 180\, p) \qquad (10)$$

where p is the period in hours, M_{p_0} is the original hardness at time zero and $\omega = 0{\cdot}01032$ for steel. From equation (7) it can be shown to a good approximation that $C \propto M^{-0{\cdot}9}$ at constant load. Substituting in (10) and re-arranging gives

$$C_{p_1}/C_{p_2} = \left[1 + \left\{\frac{\omega \log_e (p_1/p_2)}{1 - \omega \log_e 180\, p_1}\right\}\right]^{0{\cdot}9}. \qquad (11)$$

Taking $p_1 = 20$ h, $C_{p_1} = 0{\cdot}13$ W/cm^2°K, this provides a good fit to the data of Fig. 6.

The variation of conductance with heat flux was investigated next. Several values of the steady-state heat flux were used and the appropriate measurements taken, and then observations were made with the heat flux in the reverse direction across the contact. Although both specimens were of the same material a large directional effect was observed as may be

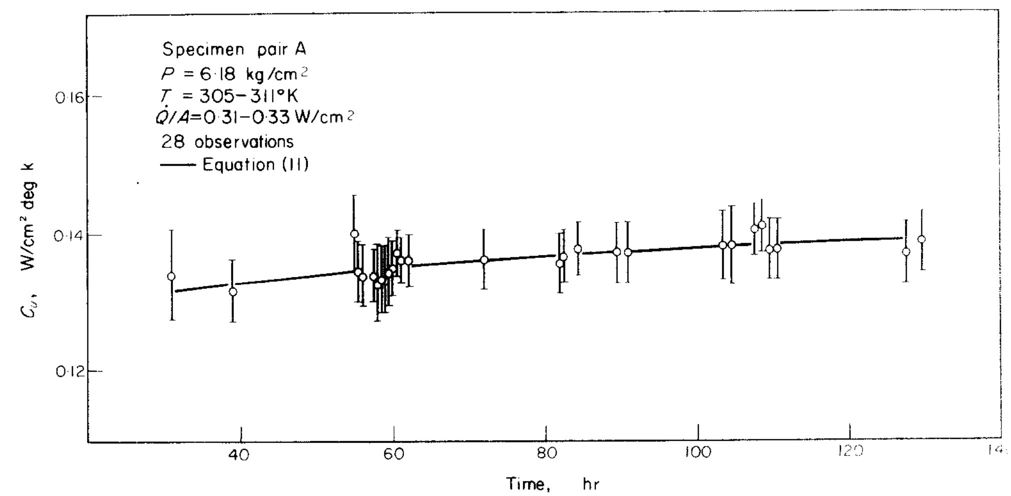

FIG. 6. Conductance of a contact vs. time.

seen in Fig. 7. The conductance however did not appear to be markedly dependent upon the magnitude of the heat flux, a sevenfold increase in heat flux producing not more than 10 per cent conductance change. Thus for the remainder of the present work, the conductance has been assumed to be invariant with the magnitude of the heat flux.

Cycling of the load, with a measurement of heat flow in each direction at each load value, failed to disclose any hysteresis within the limits error. Therefore observations made at the same load were combined in Fig. 8. Taking $E_1 = E_2 = 2\cdot0 \times 10^6$ kg/cm^2, $\nu_1 = \nu_2 = 0\cdot3$, equation (8) gives $\lambda = 8\cdot0$ with the appropriate substitutions; deformation is thus plastic and equation (7) may be applied. Agreement is not unreasonable if it is borne in mind that the theory makes no attempt to allow for the directional effect.

With liquid nitrogen in the heat sink, the first low temperature measurement was made with a downward heat flow and a reasonable result was obtained. However on reversing the direction of the heat flow, the temperature measurements when extrapolated to the interface indicated a

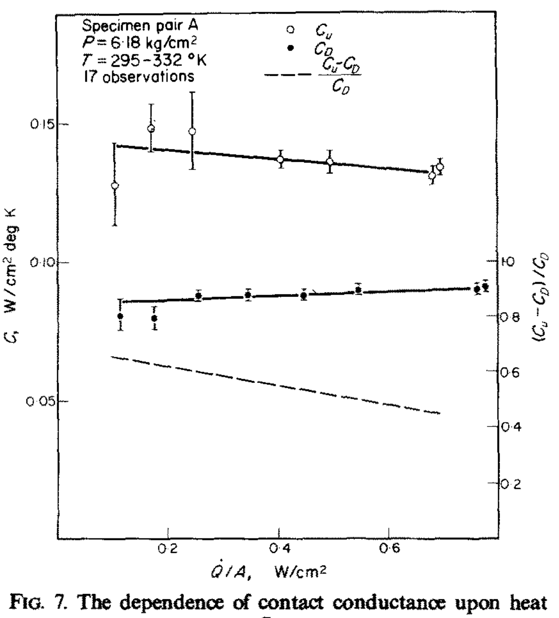

FIG. 7. The dependence of contact conductance upon heat flux.

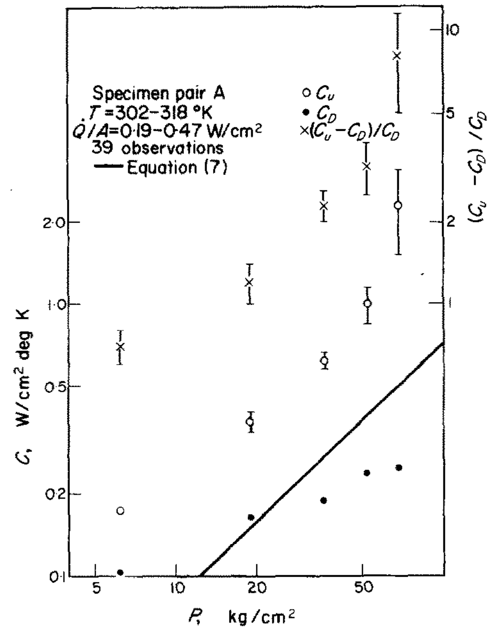

FIG. 8. Conductance behaviour with respect to load for specimen pair A contact.

negative temperature discontinuity across the contact. The measuring circuits were checked and measurements were continued at intervals over 17 h in case the effect was transient, but no change was detected. The cryostat was warmed to room temperature and recooled whereupon similar observations were obtained, despite the interim room temperature measurements indicating a positive temperature difference across the contact as expected. The temperature of the thermocouple reference junctions was changed from 77°K to 273°K and back again yet still a negative temperature difference across the contact was suggested by the measurements. Finally the cryostat was allowed to return to room temperature, the vacuum can removed, the specimens parted and the mating surfaces cleaned with organic solvent. The whole system was then reassembled and returned to liquid nitrogen temperatures. None of these procedures had any effect on the apparent negative temperature drop across the contact. To examine its variation with temperature, the cryostat was allowed to warm up to room temperature over

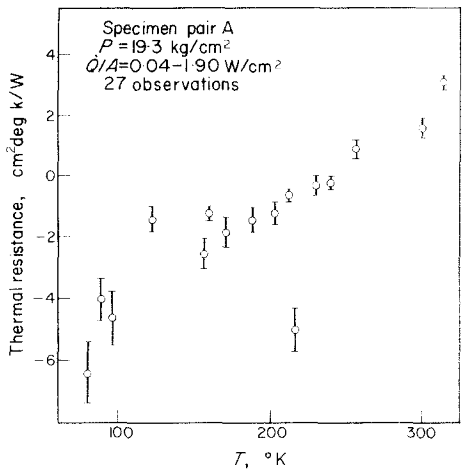

FIG. 9. Variation of thermal resistance for specimen pair A contact, under constant load, with temperature.

a period of 30 h with the heater still on, and measurements were taken at intervals. As a complete observation took less than 5 min the measurements were assumed to be those for a quasi-steady state. Results, expressed as thermal resistances, showed an approximately linear increase with temperature till they eventually went positive (see Fig. 9). Errors in the negative temperature differences due to extrapolation were often less than 10 per cent. A measurement made at liquid nitrogen temperatures in a helium atmosphere, which should have clarified the significance of any radial temperature gradients at the interface, still suggested a negative temperature difference across the contact.

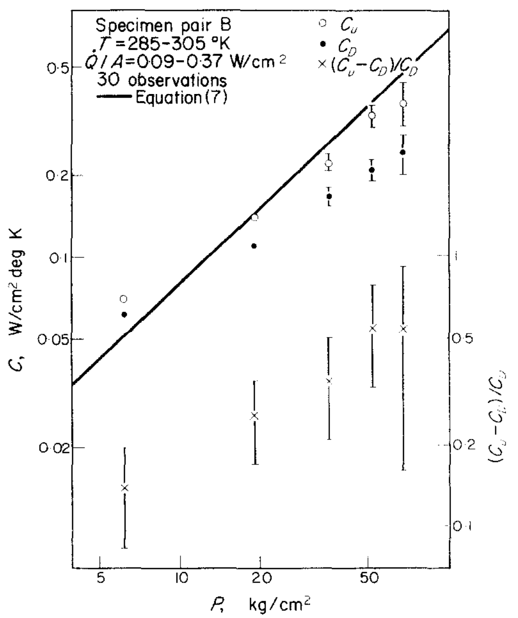

FIG. 10. Conductance behaviour with respect to load for specimen pair B contact in the temperature range 285–305°K.

Specimen pair B

Measurements were made on this specimen pair over four different temperature ranges (Figs. 10–13). As both surfaces are rough the calculation of λ requires more consideration. The expression for the plasticity index was originally derived for the contact between a set of spherically tipped asperities and a plane. For contact between two rough surfaces the necessary effective radius of curvature ρ^* is that for contact between two spheres [27], i.e.

$$1/\rho^* = 1/\bar{\rho}_1 + 1/\bar{\rho}_2 . \qquad (12)$$

This gives $\lambda = 14$ and deformation is thus plastic at room temperature. Both E and M increase with fall in temperature though not very rapidly, but this has no practical effect on the low temperature deformation as $\lambda \propto E/M$.

In order to apply equation (7), effective values of σ and $|\bar{\psi}|$ are needed. For contact between rough surfaces, Tsukizoe and Hisakado [3] suggested that $\sigma^* = \sqrt{(\sigma_1^2 + \sigma_2^2)}$, and by an argument analogous to that used by Henry [28], $\psi^* = \sqrt{(|\bar{\psi}_1|^2 + |\bar{\psi}_2|^2)}$, giving

$$\Psi = \sqrt{\left(\frac{|\bar{\psi}_1|^2 + |\bar{\psi}_2|^2}{\sigma_1^2 + \sigma_2^2}\right)} \qquad (13)$$

which leads to the surprising conclusion that the variation of conductance with load between two identical rough surfaces is the same as that between one of the surfaces and a plane. Substituting appropriate values in equation (7) gives reasonable agreement for all the results; the upward and downward conductance data

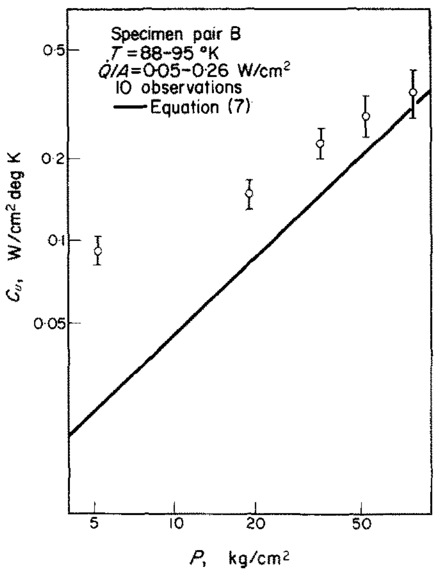

FIG. 11. Conductance of specimen pair B contact in the temperature range 88–95°K.

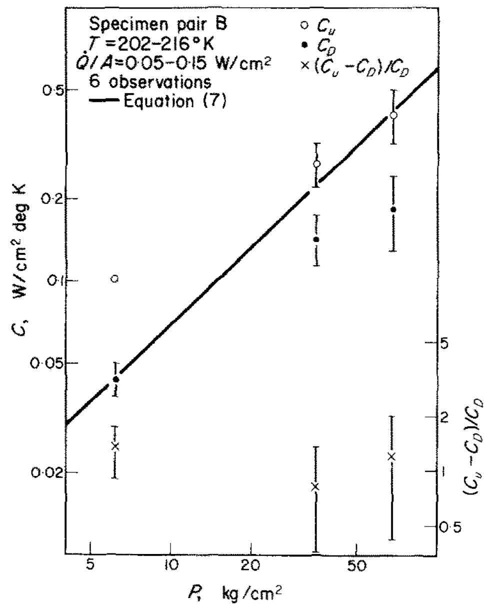

FIG. 13. Conductance of specimen pair B contact in the temperature range 202–216°K.

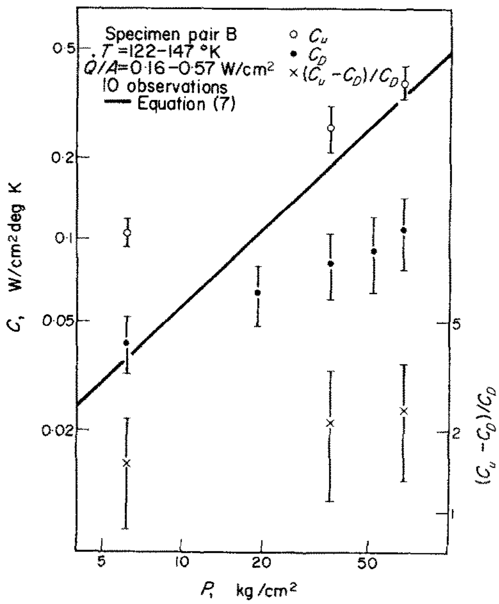

FIG. 12. Conductance of specimen pair B contact in the temperature range 122–147°K.

are fairly well bracketed but the theoretical slope is too high throughout.

It will be noted that equation (7) implies that the shape of the conductance vs. applied pressure curve is independent of all the specimen parameters: over the range of the present measurements this is true and in fact $C \propto p^{0.88}$. For a similar model, Greenwood and Williamson [29] deduced that $C \propto P^{0.9}$ approximately. A dimensionless correlation of the results has been attempted in Fig. 14: it shows that a plot of equation (7) roughly divides the upward from the downward heat flow data. A very similar correlation has been developed independently by Cooper *et al.* [30] (see Fig. 9 of that reference).

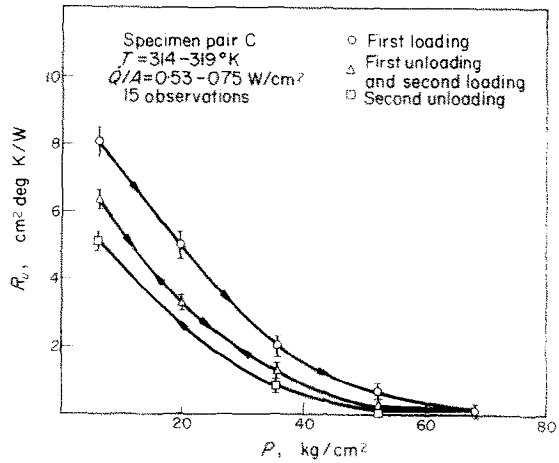

FIG. 15. Hysteresis in the thermal resistance behaviour of specimen pair C contact.

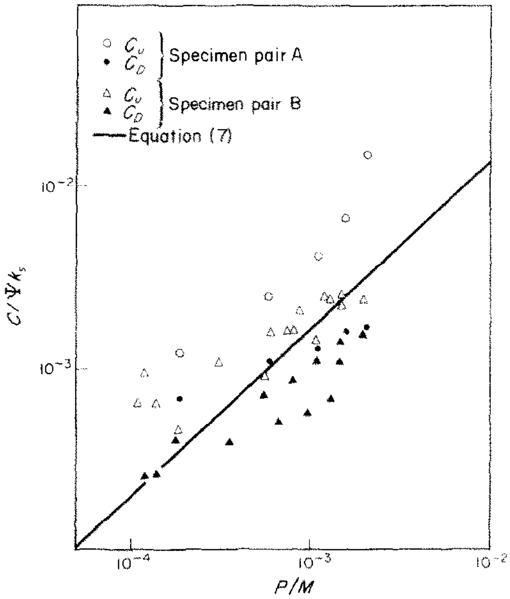

FIG. 14. Plot of a non-dimensional conductance parameter vs. a non-dimensional load parameter.

Specimen pair C

At room temperature specimen pair C was the first contact of those tested to exhibit *hysteresis* on load cycling (Fig. 15), the effect being qualitatively similar to that described by Cordier [25] and many other workers. Cordier noted that the resistances measured during the increasing and decreasing arms of the load cycles

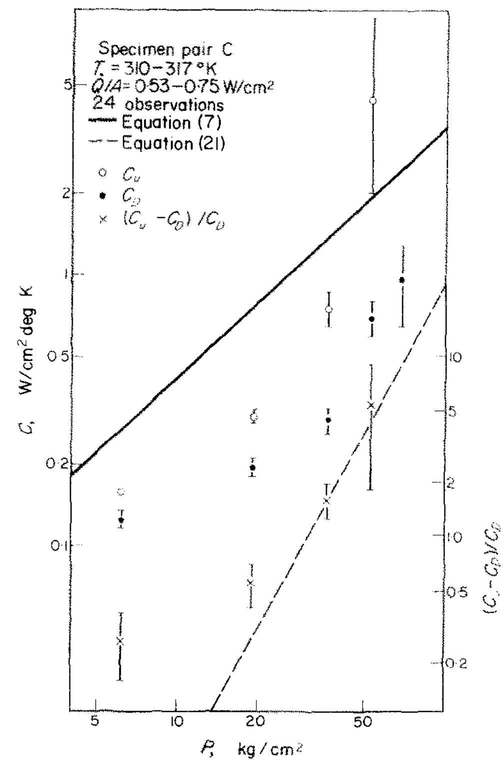

FIG. 16. Conductance behaviour with respect to load for specimen pair C contact in the temperature range 310–317°K.

tended to increase and decrease respectively with time, and suggested that if enough time were allowed to elapse between measurements, hysteresis effects would disappear; in view of the long measuring intervals in the present experiments this may explain why hysteresis was not observed with the two all-steel contacts, while pair C showed the effect because of the greater creep rate of aluminium. The middle curve of the three in Fig. 15 has been used in subsequent calculations (Fig. 16).

Measurements were also made at CO_2/acetone and liquid nitrogen temperatures (see Figs. 17 and 18). Attempts to apply the theory to these results is fraught with difficulty as the ground surface had definite directional properties due to its lay. To deduce a value for λ is out of the question, but arguments can be advanced [31] which suggest that the deformation is again plastic. Now it is shown elsewhere [20] that if β is the angle which a surface profile makes with the direction of the grinding scratches, the profile slope is given by

$$\tan \psi_\beta = \frac{\tan \psi_{\pi/2}}{\sin \alpha} \cos(\alpha - \beta) \tag{14}$$

where $\tan \alpha = \gamma$, the ratio of the long and short axes of an asperity. An effective slope ψ^* averaged over all profile directions can be found by integrating (14):

$$\psi^* = \frac{2}{\pi} \int_0^{\pi/2} \psi_\beta \, d\beta. \tag{15}$$

Taking $\gamma = 20$ and integrating graphically with $\psi_{\pi/2}$ from Table 1 gives $\psi^* = 0{\cdot}057$ rad. Substituting this and other values from Table 1 in equation (7), and remembering to use the harmonic mean thermal conductivity, gives a result which is consistently too high.

If the contact spots are treated as elliptical their constriction resistance is $f(\gamma)/2\bar{a}k_s$ [1] where $\bar{a}$ is the average radius of the ellipse.

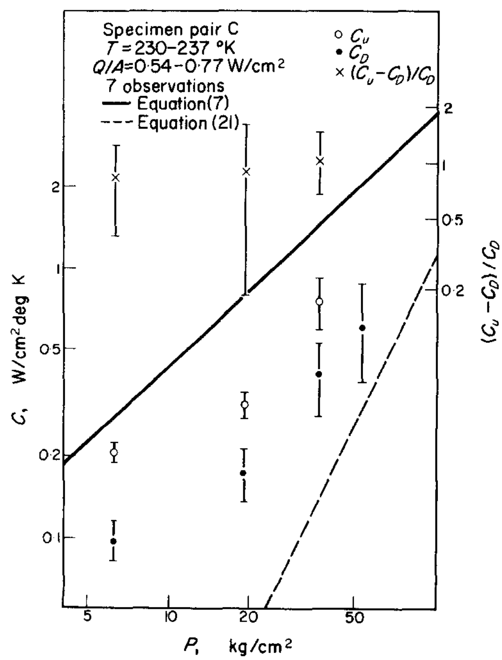

FIG. 17. Conductance of specimen pair C contact in the temperature range 230–237°K.

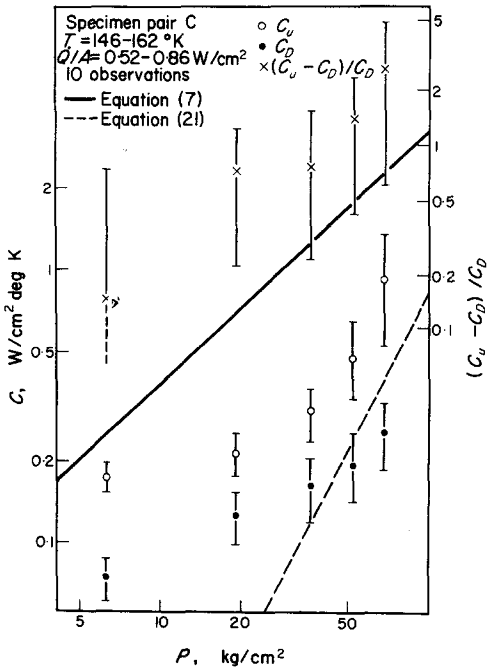

FIG. 18. Conductance of specimen pair C contact in the temperature range 146–162°K.

Now $$\bar{a} = (l_{\pi/2} \times \gamma l_{\pi/2})^{\frac{1}{2}} \tag{16}$$

where $l_{\pi/2}$ is the land length of the asperity at $\beta = \pi/2$. Hence an effective radius can be defined as

$$a^* = \frac{\sqrt{\gamma}}{f(\gamma)} l_{\pi/2}. \tag{17}$$

From equation (5) the average land length l is

$$l = \frac{2P}{M\Psi\phi(t)} \,. \tag{18}$$

If $\gamma = 20$, then $f(\gamma) = 0{\cdot}25$ [1] and $a^* = 17{\cdot}9\ l_{\pi/2}$, i.e.

$$a^* = \frac{35{\cdot}8\, P}{M\Psi_{\pi/2}\phi(t)}. \tag{19}$$

The number of contacts per unit area is difficult to deduce from any profile as the distribution is not random. Falling back on Henry's [28] assertion that for ground surfaces

$$\bar{n}_A = (\bar{n}_L)_\beta \times (\bar{n}_L)_{\beta+\pi/2}, \bar{n}_A = (\bar{n}_L)^2_{\pi/4}$$

which from equation (5)

$$= \{\Psi_{\pi/4}\, \phi(t)/2\}^2. \tag{20}$$

Combining (19) and (20) in (7) gives

$$C = 17{\cdot}9 \frac{\Psi^2_{\pi/4}}{\Psi_{\pi/2}} k_s\, \phi(t) \frac{P}{M} \,. \tag{21}$$

This represents a straight line for C vs. P of about twice the slope given by equation (7), but the predictions are now too low. The choice of γ, however, was fairly arbitrary [20]. From Dyson and Hirst's photographs [32], much higher values than 20 seem possible, and $f(\gamma)$ decreases with increasing γ: doubling γ would in fact more than double the conductance. As matters stand, equations (7) and (21) represent roughly the upper and lower limits of a band within which the conductances fall.

DIRECTIONAL EFFECT

The directional effects observed in the present series of experiments have throughout been too large to be explained by experimental errors. Also they have been characterized mainly by their lack of corroboration of previous explanations. The exhibition of such an effect between specimens of similar material verifies some of the arguments based on differential thermal expansion. The effect decreased with increasing heat flux (see Fig. 7) contrary to Clausing's findings [10]. A series of consecutive changes in heat flow direction through specimen pair A (Fig. 19) showed, if anything, an increase in directional effect with number of reversals, contrary to Williams' suggestion [11]. Increasing the pressure of the ambient gas caused no appreciable change in the directional effect (Fig. 20) although radial temperature gradients were almost eliminated, which casts doubt on explanations relying on such gradients. It should also be noted that throughout the experiments the directional effect either did not change or increased with load; this is difficult to explain on the basis of almost any geometrical theory for the effect.

As predicted by Lewis and Perkins [12] the

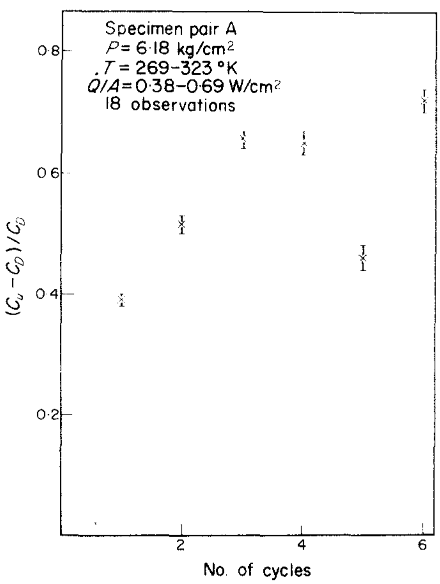

FIG. 19. The results of reversing the heat flux direction upon the thermal directional effect.

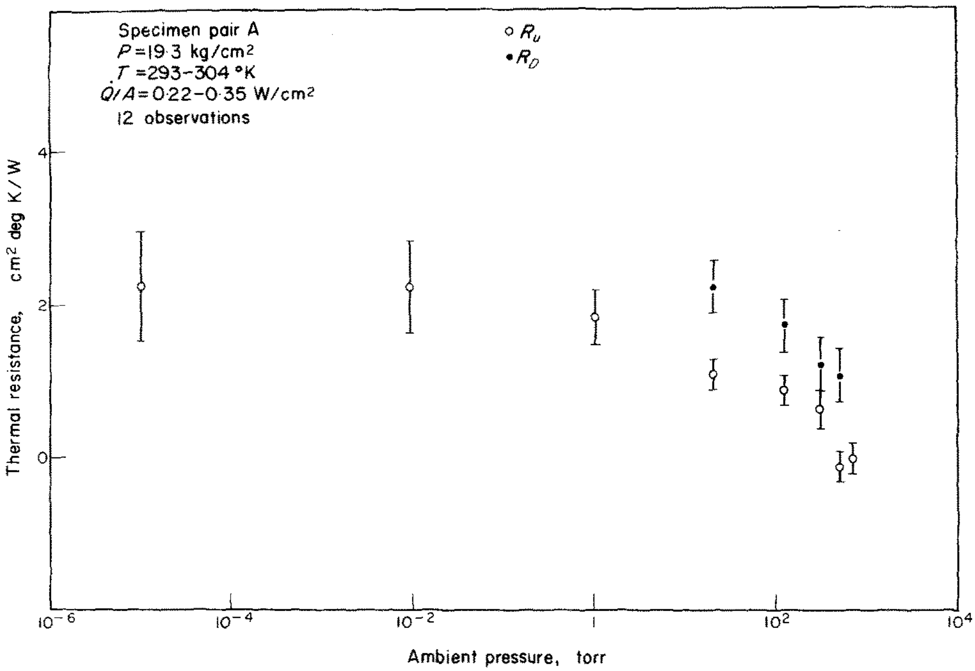

FIG. 20. Dependence of the contact resistance upon the pressure of the helium environmental gas.

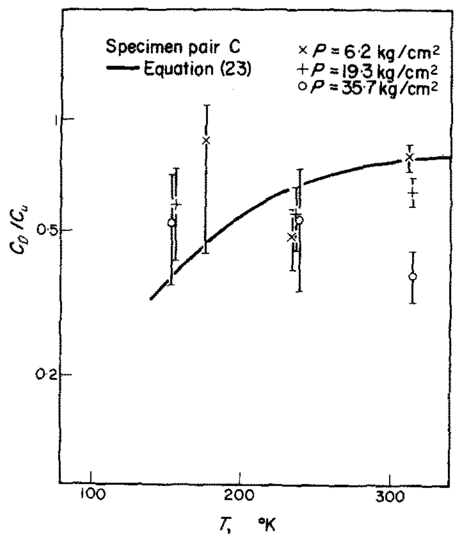

FIG. 21. Temperature dependence of the directional effect for specimen pair C contact.

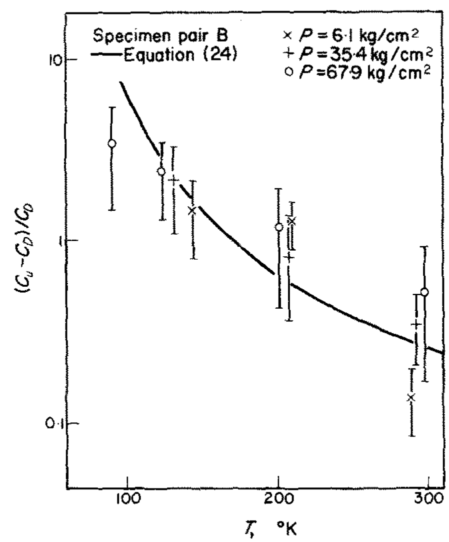

FIG. 22. Temperature dependence of the directional effect for specimen pair B contact.

contact conductance was greater when the heat flow was from the higher thermal conductivity metal—in this case aluminium to the one of lower conductivity—the stainless steel. This is the converse of what would be expected from the Clausing [10] hypothesis.

The theory which appears to hold most promise is that of Moon and Keeler [14], the main obstacle to applying it being a lack of knowledge of the work functions of the contacting surfaces. In the circumstances arbitrary values of $\Delta\varepsilon = \varepsilon_1 - \varepsilon_0$ will be assigned as follows: $\varepsilon_{AL} - \varepsilon_0 = 1{\cdot}0$ eV, $\varepsilon_{EM} - \varepsilon_0 = 0{\cdot}85$ eV. There are of plausible magnitude and chosen so that $\varepsilon_{AL} > \varepsilon_{EM}$, i.e. the conductance will be higher from aluminium to steel, in agreement with the experimental results. If $T_1 T_2 = T^2$, $T_1 - T_2 = \Delta T$ and $\tau_{12} = \tau_{21}$, equation (9) becomes

$$C_{12}/C_{21} \doteqdot \exp(\Delta\varepsilon\,\Delta T/kT^2). \tag{22}$$

Setting $\Delta\varepsilon = 1$ eV and $\Delta T = 2$°K gives

$$\log_e(C_U/C_D) = 2{\cdot}32 \times 10^4/T^2. \tag{23}$$

However comparison of this with experimental data (see Fig. 21) for specimen pair C is not very enlightening because of the large scatter in the measurements.

Although both specimens of pair B were of the same material their surface histories and hence work functions were doubtless slightly different. With this excuse $\Delta\varepsilon$ is set to 0·85 eV with the lower specimen as metal 1.
Then

$$(C_U - C_D)/C_D = \exp(1{\cdot}98 \times 10^4/T^2) - 1 \tag{24}$$

for an average ΔT of 2°K. This fits the experimental data (Fig. 22) quite well. Theory and experiment diverge at the lower end of the temperature range, but this is expected. The lattice component of the thermal conductivity of a stainless steel reaches a maximum of 30 per cent of the total conductivity at 90°K; above this temperature it falls off rapidly and heat conduction is substantially electronic [33]. Phonon heat transfer across an interface does not exhibit a directional effect [34], hence at 90°K the observed directional effect will be less than that predicted by a purely electronic theory of heat transfer.

The effect of surface changes on work functions is not well understood. It is however possible that the observed increase in directional effect with load is due to a change in the work function of, say, the oxide layer under increased pressure.

CONCLUSIONS

Bearing in mind the simplifying assumptions made, agreement between experiment and the theory based on the statistical properties of random surfaces appears quite promising. Only four parameters of each contact member need to be specified: thermal conductivity, surface hardness, RMS roughness and mean surface slope. Of these, only two are characteristic of the surface topography. The RMS roughness can conveniently be measured by commercially available instruments, and although measurement of the mean surface slope required rather elaborate techniques in the present investigation it seems likely that a simple optical method could give results of sufficient accuracy. The theory also accounts well for the variation of conductance with temperature down to 80°K. It is clear, however, that it is inadequate to describe the contact behaviour of surfaces with directional properties.

None of the geometrical theories for the directional effect advanced previously are able to give a quantitative explanation of the present results, which also conflict with many of their qualitative predictions. The theory of Moon and Keeler [14] does not suffer from so many disadvantages, and agrees well with the temperature variation of conductance of one contact.

No explanation is offered at this time for the apparent negative thermal resistance exhibited by one specimen pair.

ACKNOWLEDGEMENTS

The research was initiated and partially supported by the U.K. Atomic Energy Authority and the Science Research Council to whom we are very grateful. One of us (T.R.T.) also received personal financial support from the Welsh Plate and Sheet Manufacturers' Association.

REFERENCES

1. R. HOLM, *Electrical Contacts Handbook*, Springer-Verlag, Berlin (1958).
2. T. TSUKIZOE and T. HISAKADO, On the mechanism of contact between metal surfaces—Part I, *Trans ASME* **87D**, 666–674 (1965).
3. T. TSUKIZOE and T. HISAKADO, On the mechanism of contact between metal surfaces—Part 2, *Trans ASME* **90F**, 81–88 (1968).
4. J. A. GREENWOOD, The area of contact between rough surfaces and flats, *Trans ASME* **89F**, 81–91 (1967).
5. C. STARR, The copper oxide rectifier, *J. Appl. Phys.* **7**, 15–19 (1936).
6. M. E. BARZELAY, K. N. TONG and G. F. HOLLOWAY, Effect of pressure on the thermal conductance of contact joints, NACA Technical Note 3295 (1955).
7. G. F. C. ROGERS, Heat transfer at the interface of dissimilar metals. *Int. J. Heat Mass Transfer* **2**, 150–154 (1961).
8. A. WILLIAMS, Heat transfer at the interface of dissimilar metals, Aeronautical Research Council Report, 23, 498, strut., 2409 (1962).
9. A. WILLIAMS, An investigation into the possible rectification of heat flow across dissimilar metal contacts, Ph.D. thesis, Manchester University, England (1966).
10. A. M. CLAUSING, Heat transfer at the interface of dissimilar metals—the influence of thermal strain, *Int. J. Heat Mass Transfer* **9**, 791–801 (1966).
11. A. WILLIAMS, Comment on reference [10], *Int. J. Heat Mass Transfer* **10**, 1129–1130 (1967).
12. D. V. LEWIS and H. C. PERKINS, Heat transfer at the interface of stainless steel and aluminium—the influence of surface conditions on the directional effect, *Int. J. Heat Mass Transfer* **11**, 1371–1383 (1968).
13. J. R. BARBER, Comment on reference [10], *Int. J. Heat Mass Transfer* **11**, 617–618 (1968).
14. J. S. MOON and R. N. KEELER, A theoretical consideration of directional effects in the heat flow at the interface of dissimilar metals, *Int. J. Heat Mass Transfer* **5**, 967–971 (1962).
15. R. W. POWELL, R. P. TYE and B. W. JOLLIFFE, Heat transfer at the interface of dissimilar materials: evidence of thermal-comparator experiments, *Int. J. Heat Mass Transfer* **5**, 897–902 (1962).
16. S. D. PROBERT, T. R. THOMAS and D. WARMAN, Cryostat for measurement of heat conduction under mechanical loads, *J. Scient. Instrum.* **41**, 88–91 (1964).
17. T. R. THOMAS, S. D. PROBERT and P. W. O'CALLAGHAN, Cryostat for imposing compressive forces on contacts using an electromagnet, *J. Scient. Instrum. Ser.* 2. **2**, 282–283 (1969).
18. N. V. ZAVARITSKII, Thermal resistance of metal surfaces in contact, *J. Tech. Phys. U.S.S.R.* **21**, 453–457 (1951).
19. T. F. DURHAM, R. M. MCCLINTOCK and R. P. REED, *Cryogenic Materials Data Handbook*. U.S. Dept. of Commerce, Washington (1961).
20. T. R. THOMAS and S. D. PROBERT, Establishment of contact parameters from surface profiles, *Br. J. Appl. Phys.* (to be published March 1970).
21. H. MARGENAU and G. M. MURPHY, *The Mathematics of Physics and Chemistry*, 2nd edn, p. 519. Van Nostrand, Princeton (1956).
22. A. M. CLAUSING, Thermal contact resistance in a vacuum environment, Ph.D. thesis, University of Illinois, U.S.A. (1963).
23. F. BOESCHOTEN, On the possibility of improving the heat transfer of uranium and aluminium surfaces in contact, *Proc. Int. Conf. on Peaceful Uses of Atomic Energy* **9**, 208–209 (1955).
24. R. G. S. SKIPPER and K. J. WOOTTON, Thermal resistance between uranium and can, *Proc. 2nd Int. Conf. on Peaceful Uses of Atomic Energy* **7**, 689–690 (1958).
25. H. CORDIER, Experimental study of contact thermal resistances, *Ann. Phys.* **6**, 5–19 (1961).
26. T. N. CETINKALE and M. FISHENDEN, Thermal conductance of metal surfaces in contact, *Proc. Int. Conf. on Heat Transfer*, 271–275, I. Mech. E., London (1951).
27. S. TIMOSHENKO and J. N. GOODIER, *Theory of Elasticity*, 2nd edn, p. 372. McGraw-Hill, New York (1951).
28. J. J. HENRY, Thermal contact resistance, USAEC Report NYO 9459 (1963).
29. J. A. GREENWOOD and J. B. P. WILLIAMSON, Contact of nominally flat surfaces, *Proc. R. Soc.* **A295**, 300–319 (1966).
30. M. G. COOPER, B. B. MIKIC and M. M. YOVANOVICH, Thermal contact conductance, *Int. J. Heat Mass Transfer*, **12**, 279–300 (1969).
31. T. R. THOMAS, Thermal resistance of pressed contacts, Ph.D. thesis, University College of Swansea, Wales (1968).
32. J. DYSON and W. HIRST, The true area of contact between solids, *Proc. Phys. Soc.* **67**, 309–312 (1954).
33. R. BERMAN, Thermal conductivity of some alloys at low temperatures, *Phil. Mag.* **42**, 642–650 (1951).
34. W. A. LITTLE, The transport of heat between dissimilar solids at low temperatures, *Can. J. Phys.* **37**, 334–349 (1959).
35. A. M. CLAUSING and B. T. CHAO, Thermal contact resistance in a vacuum environment, *Trans. ASME*, **87C**, 243–251 (1965).

APPENDIX

Directional effect between specimens of similar material

Clausing [10] considered the case of two initially convex specimens of linear expansion coefficients δ_1 and δ_2. If $\delta_1 \neq 0$, $\delta_2 = 0$, and heat flows from 1 to 2, the portion of surface 1 near the contact area is colder than the rest of the surface and will contract, thus enlarging the contact area. If the heat flow is reversed, the portion of surface 1 near the contact area is now hotter than its surroundings and will expand, decreasing the contact area; hence a directional effect occurs. The argument can be extended to the case of $(\delta_1, \delta_2) \neq 0$, $\delta_1 > \delta_2$ and to a convex–concave contact. Clausing suggested that as the thermal strain is a function of the temperature gradients in the specimens the directional effect should increase with heat flux. He also believed that for specimens of the same material, i.e. $\delta_1 = \delta_2$, the thermal strain is complementary and no directional effect should appear.

Barber [13] maintained that thermal contact at a central region in the presence of radial temperature gradients is equivalent to a uniform heat source covering the central region of radius r discharging to a uniform heat sink of the same radius b as the nominal contact area. The vertical displacement of the central region would then be

$$\Delta z = \frac{\dot{Q}\delta(1+\nu)\log(b/r)}{2\pi k_s}. \tag{25}$$

He goes on to state that a thermal distortion explanation cannot account for a directional effect between similar materials, because, as the vertical displacements are equal and opposite, the conformity will remain unchanged. But consider the contact between two convex surfaces of initial radii of curvature ρ_1, ρ_2. The radius r of the area of elastic contact between them is given [27] by the Hertzian formula

$$r \propto \left(\frac{1}{\rho_1} + \frac{1}{\rho_2}\right)^{-\frac{1}{3}}. \tag{26}$$

If specimen 1 is heated and specimen 2 cooled, $\rho_1 \to (\rho_1 + \Delta\rho_1)$ and $\rho_2 \to (\rho_2 - \Delta\rho_2)$. If the heat flow is reversed keeping the magnitude of the heat flux constant, then $\rho_1 \to (\rho_1 - \Delta\rho_1)$ and $\rho_2 \to (\rho_2 + \Delta\rho_2)$. Hence

$$\left(\frac{r_{12}}{r_{21}}\right)^3 = \left(\frac{1}{\rho_1 - \Delta\rho_1} + \frac{1}{\rho_2 + \Delta\rho_2}\right)\Bigg/\left(\frac{1}{\rho_1 + \Delta\rho_1} + \frac{1}{\rho_2 - \Delta\rho_2}\right). \tag{27}$$

Rearranging and neglecting terms in $\Delta\rho_1\,\Delta\rho_2$ gives

$$\left(\frac{r_{12}}{r_{21}}\right)^3 = \left\{1 + \frac{2(\Delta\rho_2 - \Delta\rho_1)}{\rho_1 + \rho_2 + \Delta\rho_1 - \Delta\rho_2}\right\}\left\{1 + \frac{2(\rho_2\Delta\rho_1 - \rho_1\Delta\rho_2)}{\rho_1\rho_2 + \rho_1\Delta\rho_2 - \rho_2\Delta\rho_1}\right\} \tag{28}$$

$$\simeq \left\{1 + \frac{2(\Delta\rho_2 - \Delta\rho_1)}{\rho_1 + \rho_2}\right\}\left\{1 + \frac{2(\rho_2\Delta\rho_1 - \rho_1\Delta\rho_2)}{\rho_1\rho_2}\right\} \tag{29}$$

If the flatness deviation $z \ll \rho$, then

$$\frac{z}{b} \simeq \frac{b}{2\rho} \tag{30}$$

i.e.

$$\Delta\rho = -(2\rho^2/b^2)\,\Delta z \tag{31}$$

and

$$\left(\frac{r_{12}}{r_{21}}\right)^3 = \left\{1 + \frac{4}{b^2}\left(\frac{\rho_1^2\,\Delta z_1 - \rho_2^2\,\Delta z_2}{\rho_1 + \rho_2}\right)\right\}\left\{1 + \frac{4(\rho_2\Delta z_2 - \rho_1\Delta z_1)}{b^2}\right\}. \tag{32}$$

If the specimens are of the same material, $\Delta z_1 = \Delta z_2 = \Delta z$ and equation (32) reduces to

$$\left(\frac{r_{21}}{r_{21}}\right)^3 = 1 - \left\{\frac{4\Delta z(\rho_1 - \rho_2)}{b^2}\right\}^2. \tag{33}$$

Now $C \propto r$ for $r \ll b$ (e.g. see [35]), and thus $C_{12} \neq C_{21}$ for all $\rho_1 \neq \rho_2$, i.e. even if the specimens are of the same material a directional effect will be present unless the radii of curvature of the mating surfaces are identical.

RÉSISTANCE THERMIQUE DE CONTACT: L'EFFET DIRECTIONNEL ET AUTRES PROBLÈMES

Résumé—On décrit des régions mal connues dans le domaine de la résistance thermique de contact. Une théorie pour la variation de la résistance de contact avec la charge basée sur de récents progrès dans l'analyse topographique de surface est esquissée, et les théories existantes pour l'effet appelé directionnel sont discutées de façon critique. La construction et l'emploi d'un appareil pour mesurer la variation de la conductance thermique avec divers paramètres à des températures en-dessous de 300°K sont décrits, et l'on présente le résultat des combinaisons de contact de spécimens en acier inoxydable et en aluminium. L'accord entre la prévision théorique et l'observation expérimentale est bon pour des surfaces aléatoires, mais faiblit pour des surfaces orientées. Des effets directionnels ont été trouvés pour un contact entre des matériaux similaires; un essai est fait pour tenir compte de cela sur la base d'une théorie électronique antérieure pour cet effet.

THERMISCHER KONTAKT-WIDERSTAND: DER RICHTUNGSEINFLUSS UND ANDERE PROBLEME

Zusammenfassung—Noch wenig erforschte Probleme des thermischen Kontaktwiderstandes werden beschrieben. Eine Theorie für die Änderung des Kontaktwiderstandes mit dem Anpressdruck die auf kürzlich gemachten Fortschritten in der Analysis der Oberflächen-Topographie beruht, ist angegeben und die existierenden Theorien über den sogenannten Richtungseffekt wurden kritisch diskutiert. Die Konstruktion und der Gebrauch einer Apparatur zur Messung der Änderung der Leitfähigkeit bei verschiedenen Parametern und Temperaturen von 300°K abwärts wird beschrieben und die Ergebnlsse für Kontaktkombinationen von steinless-steel/Aluminium werden angegeben. Die Übereinstimmung zwischen der theoretischen Betrachtung und der experimentellen Beobachtung ist zufriedenstellend für unbearbeitete Oberflächen, ist aber nicht mehr gegeben bei Oberflächen mit Zwischenlage.

Richtungseinflüsse liessen sich für den Kontakt zwischen einzelnen Materialien finden; es wurde versucht auf Grund einer kürzlich entwickelten elektronischen Theorie den Effekt zu berücksichtigen.

ТЕРМИЧЕСКОЕ КОНТАКТНОЕ СОПРОТИВЛЕНИЕ. ЭФФЕКТ НАПРАВЛЕННОСТИ И ДРУГИЕ ПРОБЛЕМЫ

Аннотация—Статья посвящена неисследованным проблемам в области термического контактного сопротивления. Изложена теория изменения контактного сопротивления, причем основной упор сделан на последние достижения в топографическом анализе поверхности. Дан критический обзор существующих теорий так называемого эффекта направленности. Описано конструирование и использование аппарата для измерения изменений коэффициента теплопроводности при различных параметрах и температурах от 300°К и ниже, и представлены результаты для контактных комбинаций образцов нержавеющей стали и алюминия. Получено хорошее согласование теоретических расчетов с экспериментальными наблюдениями для поверхностей с неупорядоченной структурой, которое нарушается для поверхностей с упорядоченной структурой. Найдены эффекты направленности при контактировании подобных материалов. Сделана попытка учёта эффекта на основании ранее предложенной электронной теории данного эффекта.